Analytical and Bioanalytical Chemistry (2021) 413:7001–7007
https://doi.org/10.1007/s00216-021-03657-1

RESEARCH PAPER

# Ultrasensitive colorimetric strategy for $Hg^{2+}$ detection based on T-$Hg^{2+}$-T configuration and target recycling amplification

Fuming Sang[1] · Suyao Yin[1] · Jianxin Pan[1] · Zhizhou Zhang[1]

Received: 23 July 2021 / Revised: 22 August 2021 / Accepted: 9 September 2021 / Published online: 16 September 2021


## Abstract

A novelty aptasensor for ultrasensitive detection of $Hg^{2+}$ is developed, exploiting the combination of plasmonic properties of gold nanoparticles (AuNPs) and exonuclease III (Exo III)-assisted target recycling for signal amplification. In the presence of $Hg^{2+}$, a DNA duplex can be formed due to the strong coordination of $Hg^{2+}$ and T bases of single-stranded DNA (ssDNA) probe. Exo III digests the DNA duplex from the 3′ to 5′ direction, resulting in the releasing of $Hg^{2+}$. Then, the released $Hg^{2+}$ binds with another ssDNA probe through T-$Hg^{2+}$-T coordination. After Exo III-assisted $Hg^{2+}$ cycles, numerous ssDNA probes are exhausted, which promotes poly(diallyldimethylammonium chloride) (PDDA)-induced AuNP aggregation, leading to an obvious color change and aggregation-induced plasmon red shift of AuNPs (from 520 to 610 nm). Therefore, this biosensor is ultrasensitive, which is applicable to the detection of trace level of $Hg^{2+}$ with a linear range from 5 pM to 0.6 nM and an ultralow detection limit of 0.2 pM. Furthermore, it enables visual detection of $Hg^{2+}$ as low as 50 pM by the naked eye. More importantly, the assay can be applied to the reliable determination of spiked $Hg^{2+}$ in sea water samples with good recovery.

**Keywords** Colorimetry · Mercury(II) · Exonuclease III · Aptamer

## Introduction

Water-soluble $Hg^{2+}$ is one of the most toxic heavy metal ions due to its high toxicity and bioaccumulation [1, 2], which can cause serious damage to human health even at ultralow level [3]. Therefore, it is of great importance to develop a highly sensitive approach for the determination of trace amounts of $Hg^{2+}$. Many sensitive methods have been developed for $Hg^{2+}$ detection, including inductively coupled plasma mass spectroscopy (ICPMS) [4, 5], high-performance liquid chromatography (HPLC) [6, 7], atomic absorption spectroscopy (AAS) [8, 9], and atomic fluorescence spectroscopy (AFS) [10]. Nevertheless, these analytical methods are very expensive and time consuming because of the expensive instrumentation and sample pretreatment processes, which limit their widespread applications in routine $Hg^{2+}$ determination. Accordingly, it is highly demanded to develop an economical and simple method to detect $Hg^{2+}$ sensitively and specifically.

Single-stranded DNA (ssDNA) aptamers possess excellent advantages over antibodies, including cheapness, being easily synthesized, and high affinity and specificity [11–14]. In addition, $Hg^{2+}$ can specifically coordinate with the thymine (T) bases to form a T-$Hg^{2+}$-T complex [15–17]. Accordingly, a variety of methods for $Hg^{2+}$ detection based on T-$Hg^{2+}$-T interaction have been developed, such as fluorometric method [18–21], colorimetry [22–25], electrochemistry [26–28], and surface resonance Raman scattering [29]. Specially, plasmonic AuNPs-based colorimetric methods have attracted great attention thanks to their simplicity, low cost, and easy to readout by bare-eye [30–33]. Nevertheless, these colorimetric methods still suffer from the low detection sensitivity and false positive result. Therefore, many signal amplification strategies are introduced for target determination to overcome these barriers [34]. Among them, Exo III is widely used due to its low cost, highly catalytic efficiency, and easy availability [35–37]. What is more, Exo III is a sequence-independent exonuclease that can catalyze the stepwise digestion of mononucleotides from the blunt or recessed 3′ terminus of duplex DNA to recycle target molecules [38]. However, Exo III is not active on the ssDNA. Hence, Exo III-assisted target recycling amplification has been widely used in sensitive detection of biomolecules and metal ions [39–41].

✉ Fuming Sang
sangfuming@hitwh.edu.cn

[1] School of Marine Science and Technology, Harbin Institute of Technology, Weihai 264209, People's Republic of China

Herein, we firstly develop an aptasensor for ultrasensitive colorimetric detection of $Hg^{2+}$ by coupling Exo III-assisted signal amplification with PDDA-induced AuNPs aggregation. In the presence of $Hg^{2+}$, DNA duplex with blunt terminus can be formed through the formation of T-$Hg^{2+}$-T, which can be digested by Exo III from the blunt 3′ to 5′, leading to the release of $Hg^{2+}$ simultaneously. The released $Hg^{2+}$ coordinates with another new ssDNA probe and triggers a new cycle assisted with Exo III. Hence, trace amounts of $Hg^{2+}$ can lead to the digestion of a large amount of ssDNA probes into mononucleotides. Subsequently, PDDA can effectively induced the aggregation of AuNPs, exhibiting obvious color change from red to blue and the increase of the absorption ratio ($A_{610}/A_{520}$). Therefore, the proposed strategy exhibits high selectivity and greatly improved sensitivity with an ultralow detection limit of 0.2 pM. In addition, it is successfully applied to the detection of spiked $Hg^{2+}$ in sea water.

## Materials and methods

### Materials

$HAuCl_4 \cdot 4H_2O$ was bought from Sinopharm Chemical Reagent Co. Ltd (China). PDDA (MW < 100,000, 35 wt.%) was obtained from Aladdin Ltd. (China). Trisodium citrate and mercury nitrate were obtained from Laiyang Fine Chemical Plant (China). The DNA sequence (5′-TTTTGTGTGTCTGCTGTCTCACTTAT-3′) was synthesized by Sangon Biotechnology Co. Ltd. (China). Exo III was purchased from Sangon Biotechnology Co. Ltd. (China). As shown in supplementary materials, AuNPs were synthesized through the previous methods [42, 43]. All the solutions were prepared using ultrapure water (18.2 MΩ $cm^{-1}$).

### Detection procedure for $Hg^{2+}$

Probe DNA (4 μL, 1 μM), $Mg^{2+}$ (5 μL, 600 μM), and $Hg^{2+}$ with various concentrations were mixed and heated to 95 °C for 10 min, and then cooled to room temperature for 30 min. After further incubation at 37 °C for 1 h, 1 μL of 5 U/μL Exo III was added into the aforementioned mixture and incubated at 37 °C for 30 min. After that, PDDA (60 μL, 1.2 μM) was added to the above solution and incubated for 10 min at room temperature. Eventually, 200 μL AuNPs were added and followed by the addition of ultrapure water to reach a total volume 500 μL. After the incubation for 5 min, the absorption ratio ($A_{610}/A_{520}$) was obtained by a UV-vis spectrometer.

## Results and discussion

### Mechanism and feasibility

The mechanism of the colorimetric sensor for $Hg^{2+}$ detection is displayed in Scheme 1. PDDA, an excellent water-soluble cationic polymer, can effectively induce the aggregation of negatively charged AuNPs due to the electrostatic interaction, and interact with ssDNA via electrostatic attractions simultaneously. In the absence of $Hg^{2+}$, Exo III cannot digest the ssDNA probe. Therefore, the unfunctionalized AuNPs are well dispersed and exhibit wine red color in solution, stemming from the electrostatic interactions between positively charged PDDA and negatively charged ssDNA probes. However, in the presence of $Hg^{2+}$, ssDNA probe can be folded and forms a double-stranded (ds) DNA structure due to the formation of T-$Hg^{2+}$-T base pairs. Exo III digests dsDNA duplex from the blunt 3′-ends to 5′, releasing $Hg^{2+}$ from T-$Hg^{2+}$-T complex. Afterwards, the released $Hg^{2+}$ binds to another ssDNA probe and starts a new ssDNA probe digestion cycle with the assistance of Exo III. By this means, trace level $Hg^{2+}$ results in the digestion of a large amount of ssDNA probes. Consequence, anionic AuNPs are heavily aggregated by positively charged PDDA due to the electrostatic interactions with the color change from red to blue, which are then successfully applied for trace $Hg^{2+}$ visual detection. UV-vis, TEM, and DLS are used to further insight into the mechanism of the colorimetric method. As illustrated in Fig. 1a, in the absence of $Hg^{2+}$, the characteristic adsorption peak of AuNPs can be observed at about 520 nm, and the color of the solution is still red. However, in the presence of $Hg^{2+}$ (1 nM), a new absorption peak appears at 610 nm, and the absorbance at 520 nm decreases, accompanied by a color change from red to blue. TEM image (Fig. 1b) shows that

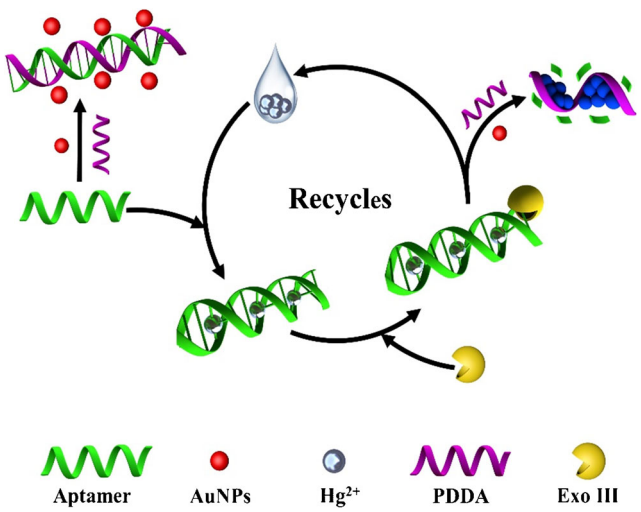


**Scheme 1** Schematic illustration of the ultrasensitive colorimetric biosensor for $Hg^{2+}$ detection based on a specific T-$Hg^{2+}$-T coordination and Exo III-aided $Hg^{2+}$ recycling amplification.

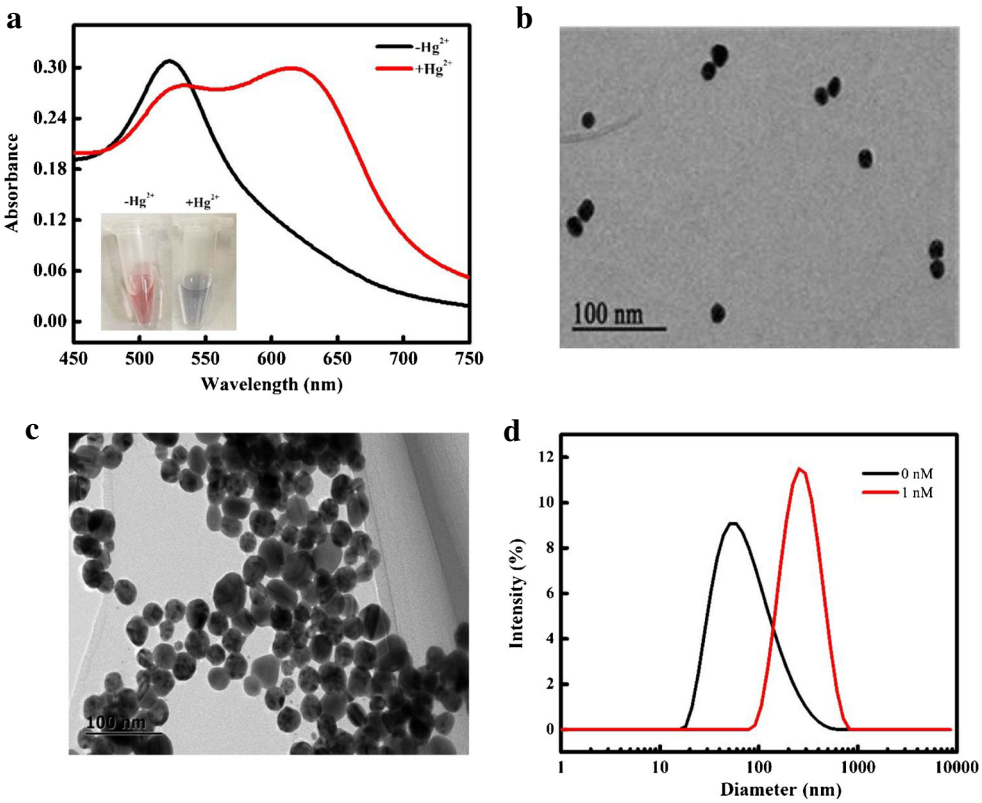


**Fig. 1** **a** UV-vis absorption spectra of the assay in the absence and presence of 1 nM $Hg^{2+}$ (insets: the corresponding photographs). **b** TEM image of AuNPs in the absence 1 nM $Hg^{2+}$. **c** TEM image of AuNPs in the presence of 1 nM $Hg^{2+}$. **d** DLS data of AuNPs in the absence and presence of 1 nM $Hg^{2+}$. Experimental conditions: 200 μL AuNPs, 1200 nM PDDA, 8 nM DNA, and 600 μM $MgCl_2$ and 5 U Exo III were used

AuNPs are uniformly dispersed in the absence of $Hg^{2+}$, indicating that the enzymatic activity Exo III is limited, whereas the presence of $Hg^{2+}$ causes AuNP aggregation (Fig. 1c), demonstrating that $Hg^{2+}$ triggered the Exo III cleavage process. Moreover, increase in the $Hg^{2+}$ concentration leads to a higher amount of aggregated AuNPs (as shown in Fig. 1c and Supplementary Information (ESM) Figure S1a). Besides, the state changes of dispersion-to-aggregation of AuNPs are authenticated by DLS data (Fig. 1d and Supplementary Information (ESM) Figure Sand Supplementary Information (ESM) Fig. S1b), which are well in agreement with TEM images.

## Optimization of experimental parameters

To attain superior sensing properties, the experimental parameters including PDDA concentration, ssDNA probe concentration, $Mg^{2+}$ concentration, incubation time, and Exo III concentration were optimized. As shown in Fig. 2a, the intensity of aggregated AuNPs increases with the increase of PDDA concentration (0 to 1600 nM). When the PDDA concentration is 1200 nM, the color of AuNPs solution changes from red to blue and the ratio of $A_{610}/A_{520}$ reaches the maximum. Hence, 1200 nM PDDA is used in the following experiments. 8 nM ssDNA probe restrains PDDA-induced aggregation of AuNPs (Fig. 2b), accompanying with a color change from blue to red. Therefore, 8 nM is selected as the optimum concentration of ssDNA probe. $Mg^{2+}$ can trigger aptamer-target specific binding [44]. Various concentrations of $MgCl_2$ were added in the absence and presence of $Hg^{2+}$, respectively. As depicted in Supplementary Information (ESM) Figure S2, the great $A_{610}/A_{520}$ difference between the blank AuNPs (without $Hg^{2+}$) and AuNPs (with $Hg^{2+}$) is observed when 600 μM $MgCl_2$ is used. Hence, the optimal concentration of $MgCl_2$ is 600 μM. The incubation time between ssDNA probe and $Hg^{2+}$ plays an important role for the sensibility. As shown in Fig. 2c, $A_{610}/A_{520}$ value reaches its maximum at 60 min. Hence, 60 min is employed for the next experiments. Exo III concentration is very important for the signal amplification. As demonstrated in Fig. 2d, the biggest $A_{610}/A_{520}$ value is attained when 5 U Exo III is added. Thus, 5 U Exo III is used for the following works.

## $Hg^{2+}$ detection

Under the optimized conditions, the sensitivity and dynamic range of the biosensor were investigated using $Hg^{2+}$ with various concentrations (0 to 1 nM). As shown in Fig. 3a, with the increase of $Hg^{2+}$ concentration, the original absorbance intensity of AuNPs at 520 nm decreases, while a new absorbance peak intense at 610 nm increases evidently. The absorption ratio values ($A_{610}/A_{520}$) versus the concentrations of $Hg^{2+}$ are plotted as Fig. 3b. Good linear relationship is observed in the $Hg^{2+}$ concentration range from 5 pM to 0.6 nM with a regression equation of $A_{610}/A_{520} = 0.92686\,[Hg^{2+}] + 0.37404$ ($R^2 = 0.998$). An ultralow limit of detection (LOD) of the assay is

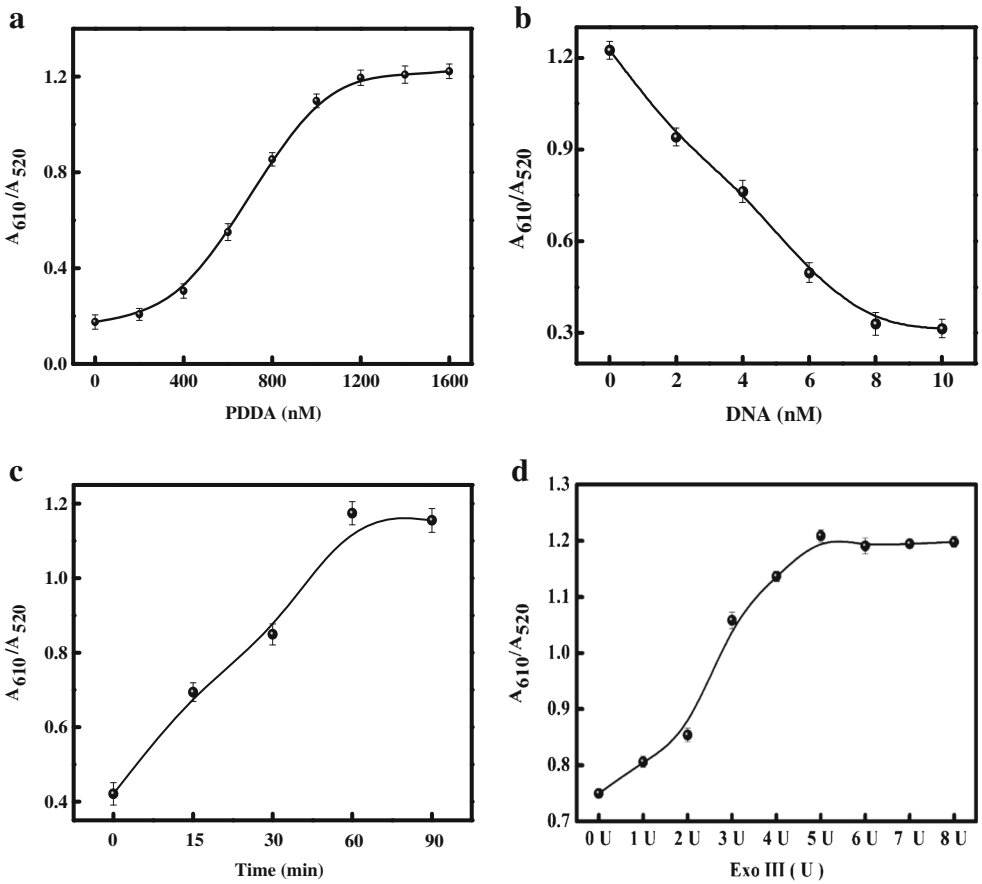


**Fig. 2** The effects of different conditions on the absorbance ratio ($A_{610}/A_{520}$). **a** PDDA concentration. **b** ssDNA probe concentration. **c** Incubation time. **d** Exo III concentration. Experimental conditions: 200 μL AuNPs and 1200 nM PDDA were used. Error bars were obtained from three experiments

calculated to be 0.2 pM using 3$\sigma$ blank/slope criteria, which is far lower than the United States EPA (USEPA) standard for $Hg^{2+}$ in drinking water (10 nM) [45], and much lower than previous reported assays (see Supplementary Information (ESM) Table S1). In addition, as indicated in Supplementary Information (ESM) Figure S3, AuNP solution color changes gradually from red to purple-blue with the increase of $Hg^{2+}$ concentration. At about 50 pM, $Hg^{2+}$ can already be detected by the naked eye, i.e., the naked eye detection limit of $Hg^{2+}$ is as low as 50 pM, which is still lower than the USEPA limit for $Hg^{2+}$ in drinking water (10 nM). Accordingly, this colorimetric assay holds enormous potential in point-of-care detection due to its naked eye readout, simple operation, and superior sensitivity.

## Selectivity

The selectivity of the colorimetric assay for $Hg^{2+}$ determination was evaluated against the interferences of glucose, citric acid, ascorbic acid, methionine, and different metal ions, including $Zn^{2+}$, $Mn^{2+}$, $Mg^{2+}$, $Na^{+}$, $Cu^{2+}$, $Ca^{2+}$, $Al^{3+}$, $Fe^{2+}$, $K^{+}$, $Ag^{+}$, $Cd^{2+}$, and $Hg^{2+}$ under the same experimental conditions.

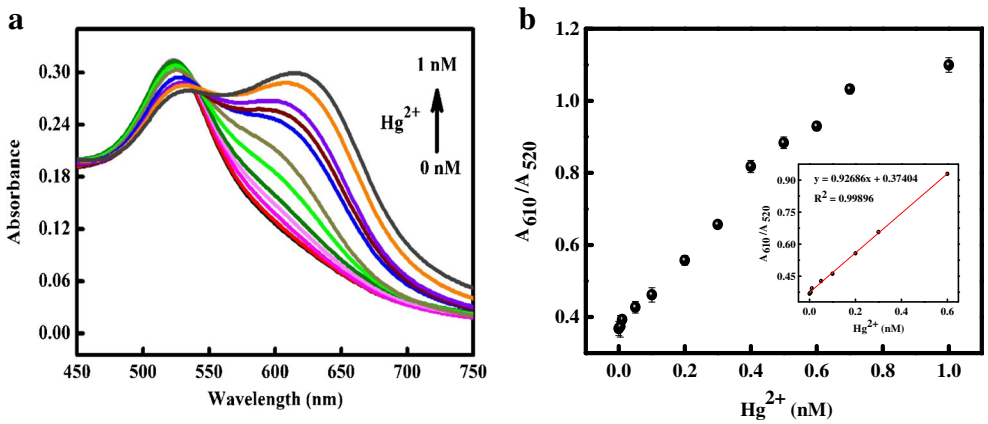


**Fig. 3** **a** UV-vis absorption spectra with various concentrations of $Hg^{2+}$ (0 to 1 nM). **b** Plot of the absorbance ratio ($A_{610}/A_{520}$) vs $Hg^{2+}$ concentration. Experimental conditions: 200 μL AuNPs, 1200 nM PDDA, 8 nM DNA, and 600 μM $MgCl_2$ and 5 U Exo III were used. Error bars were obtained from three experiments

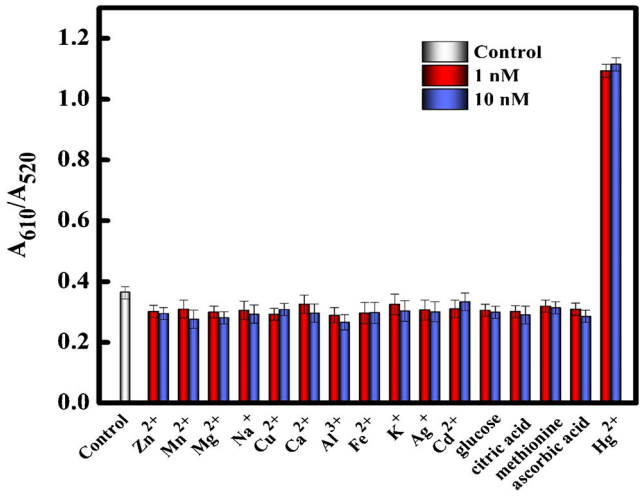


**Fig. 4** Selectivity of the colorimetric biosensor for $Hg^{2+}$ over other metal ions. Experimental conditions: 200 μL AuNPs, 1200 nM PDDA, 8 nM DNA, and 600 μM $MgCl_2$ and 5 U Exo III were used. Error bars were obtained from three experiments

As shown in Fig. 4, only $Hg^{2+}$ exhibits a significant high ratio value of $A_{610}/A_{520}$ indicating complete aggregation of AuNPs. While the other related species with two different concentrations of 1 nM and 10 nM do not elicit any significant change compared to the control. The results demonstrate the excellent selectivity of the biosensor for $Hg^{2+}$, which is attributed to the specific coordination of T-$Hg^{2+}$-T base pairs and the preferential endonuclease activity of Exo III.

## Real sample analysis

To validate the practical applicability of the assay, we used it to detect $Hg^{2+}$ in real sea water. The sea water was filtered through a 0.45-μM filter prior to measurement. $Hg^{2+}$ was spiked into the sea water with various concentrations and analyzed using the present biosensor. The results are shown in Table 1. Satisfactory recoveries between 97.20 and 103.90% are observed, which further demonstrate that the possible interference from the sea water samples on the biosensor assay can be negligible.

**Table 1** Determination of spiked $Hg^{2+}$ in sea water samples using the colorimetric biosensor

| Add $Hg^{2+}$ (nM) | Measured $Hg^{2+}$ (nM) | Recovery (%) | RSD ($n$=3) |
|---|---|---|---|
| 0.5 | 0.486 | 97.20 | 2.84 |
| | 0.492 | 98.40 | |
| | 0.513 | 102.60 | |
| 0.1 | 0.1012 | 101.20 | 2.41 |
| | 0.1039 | 103.90 | |
| | 0.0991 | 99.10 | |

## Conclusion

In summary, a colorimetric assay is successfully developed for visual detection of $Hg^{2+}$ based on T-$Hg^{2+}$-T coordination and Exo III-assisted signal amplification. Due to the Exo III-assisted target recycling strategy, the assay can be ultrasensitive detection of $Hg^{2+}$, with a low detection limit of 0.2 pM. In addition, the assay has been successfully applied in the detection of $Hg^{2+}$ in sea water with high selectivity. More importantly, no expensive instruments and reagents are used. Therefore, it is a very promising strategy for monitoring detection of $Hg^{2+}$ in point-of-care applications where $Hg^{2+}$ concentration is extremely low.

**Supplementary Information** The online version contains supplementary material available at https://doi.org/10.1007/s00216-021-03657-1.

**Funding** This work was funded by the Natural Science Foundation of China (NSFC) (No. 21407035), Shandong Provincial Natural Science Foundation (ZR2014BM021), Technology and Development Program of Weihai (2014DXGJ15), and HIT-NSRIF (2011101).

## Declarations

**Conflict of interest** The authors declare no competing interests.

## References

1. Yao L, Gao S, Liu S, Bi Y, Zheng L. Single-atom enzyme functionalized solution-gated graphene transistor for real-time detection of mercury ion. ACS Appl Mater Interfaces. 2020;12(5):6268–75.
2. Harris HH, Pickering IJ, George GN. The chemical form of mercury in fish. Science. 2003;301(5637):1203.
3. Wu H, Tong C. Dual-emission fluorescent probe for the simultaneous detection of nitrite and mercury (II) in environmental water samples based on the $Tb^{3+}$-modified carbon quantum dot/3-aminophenylboronic acid hybrid. Anal Chem. 2020;92(13):8859–66.
4. Rahman GM, Wolle MM, Fahrenholz T, Kingston HS, Pamuku M. Measurement of mercury species in whole blood using speciated isotope dilution methodology integrated with microwave-enhanced solubilization and spike equilibration, headspace–solid-phase microextraction, and GC-ICP-MS analysis. Anal Chem. 2014;86(12):6130–7.
5. Chen X, Han C, Cheng H, Wang Y, Liu J, Xu Z, et al. Rapid speciation analysis of mercury in seawater and marine fish by cation exchange chromatography hyphenated with inductively coupled plasma mass spectrometry. J Chromatogr A. 2013;1314:86–93.
6. Gao Z, Ma X. Speciation analysis of mercury in water samples using dispersive liquid-liquid microextraction combined with high-performance liquid chromatography. Anal Chim Acta. 2011;702(1):50–5.
7. Yuan Y, Wu Y, Wang H, Tong Y, Sheng X, Sun Y, et al. Simultaneous enrichment and determination of cadmium and mercury ions using magnetic PAMAM dendrimers as the adsorbents for magnetic solid phase extraction coupled with high performance liquid chromatography. J Hazard Mater. 2020;386:121658.

8. Butler OT, Cairns W, Cook JM, Davidson CM. Atomic spectrometry update. Environmental analysis. J Anal At Spectrom. 2012;26:187–221.
9. Martinis EM, Bertón P, Olsina RA, Altamirano JC, Wuilloud RG. Trace mercury determination in drinking and natural water samples by room temperature ionic liquid based-preconcentration and flow injection-cold vapor atomic absorption spectrometry. J Hazard Mater. 2009;167(1–3):475–81.
10. Song C, Zhang Y, Li X, Ouyang G, Cui J, Zhang L, et al. Morphology-maintaining synthesis of copper hydroxy phosphate@metal–organic framework composite for extraction and determination of trace mercury in rice. Food Chem. 2021;343:128508.
11. Ma Y, Geng F, Wang Y, Xu M, Shao C, Qu P, et al. Novel strategy to improve the sensing performances of split ATP aptamer based fluorescent indicator displacement assay through enhanced molecular recognition. Biosens Bioelectron. 2019;134:36–41.
12. Kolm C, Cervenka I, Aschl UJ, Baumann N, Jakwerth S, Krska R, et al. DNA aptamers against bacterial cells can be efficiently selected by a SELEX process using state-of-the art qPCR and ultra-deep sequencing. Sci Rep. 2020;10(1):20917.
13. Li H, Chang J, Gai P, Feng L. Label-free and ultrasensitive biomolecule detection based on aggregation induced emission fluorogen via target-triggered hemin/G-quadruplex-catalyzed oxidation reaction. ACS Appl Mater Interfaces. 2018;10(5):4561–8.
14. Wang X, Lv W, Wu J, Li H, Li F. In situ generated nanozyme-initiated cascade reaction for amplified surface plasmon resonance sensing. Chem Commun. 2020;56(33):4571–4.
15. Ono A, Togashi H. Highly selective oligonucleotide-based sensor for mercury(II) in aqueous solutions. Angew Chem Int Ed Eng. 2004;43:4300–2.
16. Miyake Y, Togashi H, Tashiro M, Yamaguchi H, Oda S, Kudo M, et al. Mercury$^{II}$-mediated formation of thymine-Hg$^{II}$-thymine base pairs in DNA duplexes. J Am Chem Soc. 2006;128(7):2172–3.
17. Tanaka Y, Oda S, Yamaguchi H, Kondo Y, Kojima C, Ono A. $^{15}$N-$^{15}$N J-coupling across Hg$^{II}$: direct observation of Hg$^{II}$-mediated T-T base pairs in a DNA duplex. J Am Chem Soc. 2007;129(2):244–5.
18. Wang S, Lin B, Chen L, Li N, Xu J, Wang J, et al. Branch-migration based fluorescent probe for highly sensitive detection of mercury. Anal Chem. 2018;90(20):11764–9.
19. Li Z, Sun H, Ma X, Su R, Sun R, Yang C, et al. Label-free fluorescence "turn-on" strategy for mercury (II) detection based on the T-Hg$^{2+}$-T configuration and the DNA-sensitized luminescence of terbium (III). Anal Chim Acta. 2020;1099:136–44.
20. Kong RM, Ma L, Han X, Ma C, Qu F, Xia L. Hg$^{2+}$-mediated stabilization of G-triplex based molecular beacon for label-free fluorescence detection of Hg$^{2+}$, reduced glutathione, and glutathione reductase activity. Spectrochim Acta A Mol Biomol Spectrosc. 2020;228:117855.
21. Hu PP, Liu N, Wu KY, Zhai LY, Xie BP, Sun B, et al. Successive and specific detection of Hg$^{2+}$ and I$^-$ by a DNA@MOF biosensor: experimental and simulation studies. Inorg Chem. 2018;57(14):8382–9.
22. Chen J, Pan J, Shu C. A naked-eye colorimetric sensor for Hg$^{2+}$ monitoring with cascade signal amplification based on target-induced conjunction of split DNAzyme fragments. Chem Commun. 2017;53(73):10224–7.
23. Li X, Du Z, Lin S, Tian J, Tian H, Xu W. Exo III and TdT dependent isothermal amplification (ETDA) colorimetric biosensor for ultra-sensitive detection of Hg$^{2+}$. Food Chem. 2020;316:126980.
24. Memon AG, Zhou X, Liu J, Wang R, Liu L, Yu B, et al. Utilization of unmodified gold nanoparticles for label-free detection of mercury (II): insight into rational design of mercury-specific oligonucleotides. J Hazard Mater. 2017;321:417–23.
25. Xing Y, Zhu Q, Zhou X, Qi P. A gold nanoparticle-based colorimetric mercury(II) biosensor using a DNA probe with phosphorothioate RNA modification and exonuclease III-assisted signal amplification. Microchim Acta. 2020;187(4):1–8.
26. Bala A, Górski Ł. Peptide nucleic acid as a selective recognition element for electrochemical determination of Hg$^{2+}$. Bioelectrochemistry. 2017;119:189–95.
27. Xiong E, Wu L, Zhou J, Yu P, Zhang X, Chen J. A ratiometric electrochemical biosensor for sensitive detection of Hg$^{2+}$ based on thymine-Hg$^{2+}$-thymine structure. Anal Chim Acta. 2015;853:242–8.
28. Ma N, Ren X, Wang H, Kuang X, Fan D, Wu D, et al. Ultrasensitive controlled release aptasensor using thymine-Hg$^{2+}$-thymine mismatch as a molecular switch for Hg$^{2+}$ detection. Anal Chem. 2020;92(20):14069–75.
29. Zhang L, Chang H, Hirata A, Wu H, Xue QK, Chen M. Nanoporous gold based optical sensor for sub-ppt detection of mercury ions. ACS Nano. 2013;7(5):4595–600.
30. Liu CW, Hsieh YT, Huang CC, Lin ZH, Chang HT. Detection of mercury(II) based on Hg$^{2+}$-DNA complexes inducing the aggregation of gold nanoparticles. Chem Commun. 2008;19:11764–9.
31. Memon AG, Xing Y, Zhou X, Wang R, Liu L, Zeng S, et al. Ultrasensitive colorimetric aptasensor for Hg$^{2+}$ detection using Exo-III assisted target recycling amplification and unmodified AuNPs as indicators. J Hazard Mater. 2020;384:120948.
32. Song X, Wang Y, Liu S, Zhang X, Wang H, Wang J, et al. Colorimetric and visual mercury(II) assay based on target-induced cyclic enzymatic amplification, thymine-Hg(II)-thymine interaction, and aggregation of gold nanoparticles. Microchim Acta. 2019;186(2):1–7.
33. Zhu Y, Cai Y, Zhu Y, Zheng L, Ding J, Quan Y, et al. Highly sensitive colorimetric sensor for Hg$^{2+}$ detection based on cationic polymer/DNA interaction. Biosens Bioelectron. 2015;69:174–8.
34. Gu C, Kong X, Liu X, Gai P, Feng L. Enzymatic biofuel-cell-based self-powered biosensor integrated with DNA amplification strategy for ultrasensitive detection of single-nucleotide polymorphism. Anal Chem. 2019;91(13):8697–704.
35. Yu L, Wei L, Hui X, Hou C, Bai L, Wang W. Label-free detection of Hg$^{2+}$ based on Hg$^{2+}$-triggered toehold binding, exonuclease III assisted target recycling and hybridization chain reaction. Sensor Actuat B-Chem. 2017;248:411–8.
36. Gan X, Zhao H, Chen S, Quan X. Electrochemical DNA sensor for specific detection of picomolar Hg(II) based on exonuclease III-assisted recycling signal amplification. Analyst. 2015;140(6):2029–36.
37. Liu S, Lin Y, Wang L, Liu T, Cheng C, Wei W, et al. Exonuclease III-aided autocatalytic DNA biosensing platform for immobilization-free and ultrasensitive electrochemical detection of nucleic acid and protein. Anal Chem. 2014;86(8):4008–15.
38. Zuo X, Xia F, Xiao Y, Plaxco KW. Sensitive and selective amplified fluorescence DNA detection based on exonuclease III-aided target recycling. J Am Chem Soc. 2010;132(6):1816–8.
39. Zhao Y, Gao XY, Wang H, Wang J, Zhou J, Zhao W, et al. Ultrasensitive detection of microRNA via a Au@Ag nanosnowman. Anal Chem. 2019;91(24):15988–92.
40. Feng Q, Qin L, Wang M, Wang P. Signal-on electrochemical detection of DNA methylation based on the target-induced conformational change of a DNA probe and exonuclease III-assisted target recycling. Biosens Bioelectron. 2020;149:111847.
41. Song X, Yu W, Su L, Xue Z, Wang H, Wang J, et al. Ultrasensitive electrochemical detection of Hg$^{2+}$ based on an Hg$^{2+}$-triggered exonuclease III-assisted target recycling strategy. Analyst. 2018;143(23):4008–15.
42. Sang F, Yin S, Pan J, Liu D, Zhang Z. Colorimetric determination of DNA using an aptamer and plasmonic nanoplatform. Microchim Acta. 2020;187(7):1–7.

43. Sang F, Zhang X, Liu J, Yin S, Zhang Z. A label-free hairpin aptamer probe for colorimetric detection of adenosine triphosphate based on the anti-aggregation of gold nanoparticles. Spectrochim Acta A Mol Biomol Spectrosc. 2019;217:122–7.
44. Sang F, Liu J, Zhang X, Pan J. An aptamer-based colorimetric Pt (II) assay based on the use of gold nanoparticles and a cationic polymer. Microchim Acta. 2018;185(5):1–8.
45. Zhang Y, Xiao JY, Zhu Y, Tian LJ, Wang WK, Zhu TT, et al. A fluorescence sensor based on biosynthetic CdSe/CdS quantum dots and liposome carrier signal amplification for mercury detection. Anal Chem. 2020;92(5):3990–7.